Fabrication and characterization of direct-written 3D TiO_2 woodpile electromagnetic bandgap structures

Li Ji-Jiao(李吉皎)[a], Li Bo(李 勃)[a,†], Peng Qin-Mei(彭琴梅)[a], Zhou Ji(周 济)[b], and Li Long-Tu(李龙土)[b]

[a] *Graduate School at Shenzhen, Tsinghua University, Shenzhen* 518055, *China*

[b] *State Key Laboratory of New Ceramics and Fine Processing, School of Materials Science and Engineering, Tsinghua University, Beijing* 100084, *China*

(Received 18 March 2014; revised manuscript received 4 May 2014; published online 16 July 2014)

Three groups of three-dimensional (3D) TiO_2 woodpile electromagnetic gap materials with tailed rheological properties were developed for direct-written fabrication. Appropriate amount of polyethyleneimine (PEI) dispersants allow the preparation of TiO_2 inks with a high solid content of 42 vol.%, which enables them to flow through the nozzles easily. The inks exhibit pseudoplastic behavior. The measured microwave characteristics of the results agree well with simulations based on plane wave expansion (PWE).

Keywords: TiO_2, woodpile structure, direct writing

PACS: 81.16.Dn, 83.60.Fg, 83.80.Hj, 81.05.−t **DOI:** 10.1088/1674-1056/23/9/098104

1. Introduction

Traditional methods for fabricating a TiO_2 apparatus or appliance need expensive, time-consuming molds for the products. However, direct-writing[1–3] or robocasting, controlled by a computer, offers an alternative without molds. The design of the structure can be delivered through a program in the computer. While the direct-writing technique is versatile, the most difficult and challenging part is the preparation of the desired inks. Two criteria have to be satisfied. First, the inks must behave like pseudoplastic fluids, possessing a high storage modulus with a high yield stress. Second, the inks should keep a certain shape immediately after being extruded. To meet these conditions, the greater the solid loading of the inks, the better. With high concentration, the shrinkage and defects will be less.

Out of all the diverse structures which can be deposited through direct-writing or robocasting, one novel structure proposed by Lin is called a "woodpile".[4–6] The woodpile lattice is one of the most popular three-dimensional (3D) lattice structures. Rods with a high aspect ratio are built in layers. In the first layer, the rods are arranged in parallel. The spacing distance between every two rods is constant. Then, the second layer is perpendicular to the first layer, whereas the third layer is parallel to the first, but staggers half the spacing distance. Again, the fourth layer is parallel to the second, and staggers half the spacing distance. A unit is comprised of these four layers. The main structures of three-dimensional photonic crystals are inverse opal structure, diamond structure, and woodpile structure. Among these three structures, a lot of laboratory research has been done about inverse opal structure by commonly self-assembly using an FCC template, after which the opal structure is made. However, the FCC structures will not have completely forbidden band due to a high symmetry energy level degeneracy. Structures of diamond and the woodpile structure can create a relatively wide photonic band gap. The optimized woodpile structure can give rise to a wider photonic band gap. Woodpile structure with face-centered-tetragonal (FCT) symmetry is more likely to have a wide photonic band gap relative to the FCC, because symmetry is reduced. TiO_2 has many applications in solar cells,[7] photocatalytic activity,[8] radar absorbent coatings,[9] and one-dimensional photonic crystals.[10] Until now, no 3D woodpile TiO_2 structure with electrical properties has been demonstrated.

In this letter, we report our fabrication of TiO_2 inks suitable for direct-writing and analyze the gap characteristics of 3D woodpile structures with face-centered-tetragonal (FCT) symmetry with three different spacing distances. The electronic properties of the materials are investigated experimentally and theoretically. All these results provide useful guidance for the design of 3D functional devices and offer significant clues toward the optimization of such direct-write assembled structures.

2. Experimental procedure

2.1. Materials system

Anatase titanium dioxide (TiO_2) (China National Medicines Corporation Ltd., Beijing, China) served as the ceramic phase. Surface area of powder was tested on a quantachrome instrument (Quantachrome Quadra WinQuadraSorb SI 2000-07). PEI (99%, $M_w = 600$ g/mol and

†Corresponding author. E-mail: boli@mail.tsinghua.edu.cn

© 2014 Chinese Physical Society and IOP Publishing Ltd

$M_w = 1200$ g/mol, Aladdin Industrial Corporation, Shanghai, China), which was used as the dispersing agent, was prepared in aqueous stock solutions with 10 wt.%. An aqueous solution of the ammonium salt of poly (acrylic acid) (PAA) (Darvan 821A, R.T. Vanderbilt Co., Norwalk, CT) was used as a flocculating agent. Aqueous phase pH adjustments were made by using NH_4OH (23%–28%, Beijing Modern Oriental Fine Chemical Co., Ltd., Beijing, China). All samples were prepared in de-ionized water.

2.2. Ink preparation

TiO_2 inks were prepared by making a stable suspension in deionized water, the pH value of which was first adjusted to around 9.5 by 1M NH_4OH. An appropriate amount of PEI was added into the bottle. The solution was placed in a paint shaker for 10 minutes to be well mixed. Then the powder was added step by step, during each step the suspension was shaken for 20 minutes. The gel was mixed again for 30 minutes before the addition of Darvan (PAA) (2.0 wt.% by weight of TiO_2 power).

2.3. Zeta potential and pH Values

Zeta potential (ξ) measurements were carried out for pure TiO_2 and TiO_2-PEI suspensions (volume fraction $\phi = 0.013$) as a function of pH on colloidal dynamics zeta probe (Colloidal Dynamics LLC, FL, USA).

2.4. Rheological properties

The shear elastic modulus and the shear flow behavior were measured for colloidal gel inks using a MCR300 advanced rheometer (Physica MRC300 Modular Compact Rheometer, Germany). After loading inks into the measuring system, an equilibration time of 1800 s was observed prior to each measurement. The apparent viscosity (η_{app}) of the ink was measured as a function of shear rate ($\dot{\gamma} = 0.1$ to 110 s^{-1}) in an ascending order. Oscillation measurements were performed at a frequency of 1 Hz to detect the storage modulus (G') and loss modulus (G''), where an ascending stress sweep ($\tau = 55$ to 1000 Pa) was applied. To minimize the influence of the previous measurement, we set the waiting time to be 15 s for the measurements of shear elastic modulus and 30 s for the shear flow. All measurements were carried out at a constant temperature of 25 °C.

2.5. Fabrication of 3D structures

The ink was loaded into a syringe and extruded through nozzles with different sizes, ranging from 100 μm to 2 mm. After finishing the first layer in the x–y plane, the nozzle was lifted in the z direction and continued the second layer until the total 3D object is done. Each sample comprised of 8 layers.

2.6. Sintering of samples

The as-constructed samples were dried under ambient conditions for 48 hours to evaporate water first. Then organics were eliminated by putting the dried sample in an oven, where the temperature was increased to 600 °C at a rate of 5 °C/min. After 4 hours, the temperature was raised to 1230 °C at 2.6 °C/min and maintained for another 4 hours. After that it was cooled down to 1000 °C at 2 °C/min and maintained for 2 hours, followed by cooling in natural air.

2.7. Morphology measurement

The crystalline phases were investigated by X-ray diffractometer (Shimadzu Diffractometer, Japan) and morphology by a scanning electron microscope (JEOL JSM-7001, Tokyo, Japan).

2.8. Dielectric measurement

Some bulk cylinders along with the 3D structures were sintered in the furnace. Electrodes were fabricated on both sides using conductive Ag paste. Samples were then placed into a conductivity jig and measured by HP4192A (Hewlett-Packard Company, Santa Clara, California, USA) for electrical property measurement ranging from 40 Hz to 110 MHz.

2.9. Electronic measurement

A network analyzer (HP8720ES) was used to measure transmission properties. The electromagnetic band gap profiles of three woodpile structures were calculated based on plane wave expansion (PWE).

3. Results and discussion

The morphology and average particle size distribution of the original powder is shown in Fig. 1. D50 is 1.43 μm. The XRD result of the original TiO_2 powder is of anatase type, which is illustrated in Fig. 2. The as-received powder exhibited a poor performance,[11] and its morphology would influence the later reaction, so it is pre-sintered for 4 hours at 750 °C. After pre-sintering, the phase is the same as that of the original powder shown in Fig. 2. No phase transition occurs at 750 °C. However, after sintering at 1230 °C for 4 hours, the anatase TiO_2 changes to rutile TiO_2 and owing to the pre-sintering, surface area is 7.796 m^2/g, which lies in a range suitable for robocasting.

Figure 3 shows the viscosity coated with PAA, PEI ($M_w =$ 600 g/mol), PEI ($M_w = 1200$ g/mol) at different concentrations as a function of shear rate. This indicates that the three polyelectrolytes display similar behavior: the viscosity decreases with increasing shear rate. Though the viscosity of slurry with PAA is much smaller than PEI, PEI is chosen to

coat the TiO_2. The PEI is a popular cationic polymer used in direct writing,[12] which enables the inks to exhibit high gel strength. As illustrated in Fig. 3(a), when the concentration of PAA reaches 2.34 wt.%, viscosity is maximized. However, it is observed that the slurry with PEI_{600} has a lower viscosity as the concentration increases, similar to PEI_{1200}. Only PEI concentrations beyond saturation adsorption could perceptively improve the stability of TiO_2 suspensions, which is the same as other researcher's results.[13,14] PEI forms an ionically cross-linked network while PAA possess a much lower molecular weight and highly branched nature.[15] There is no significant viscosity difference among different concentrations for PEI, but the shear modulus is different.[12]

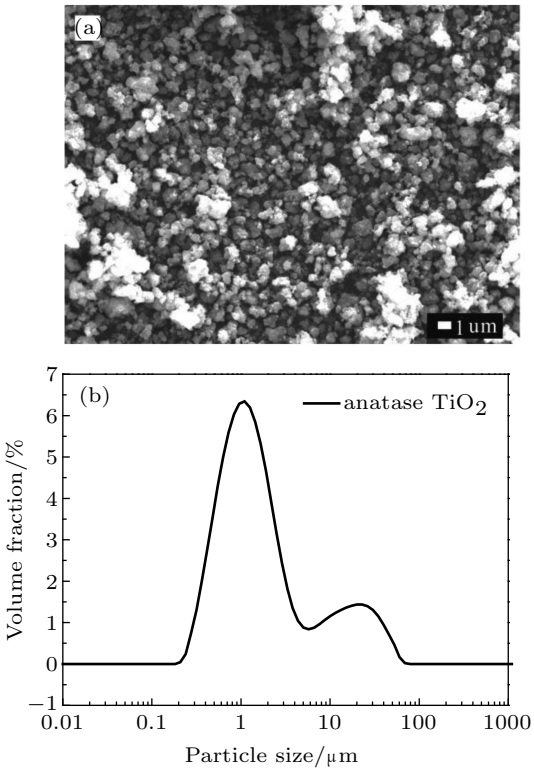


Fig. 1. (a) Morphology of pre-sintered powder; (b) TiO_2 particle size distribution.

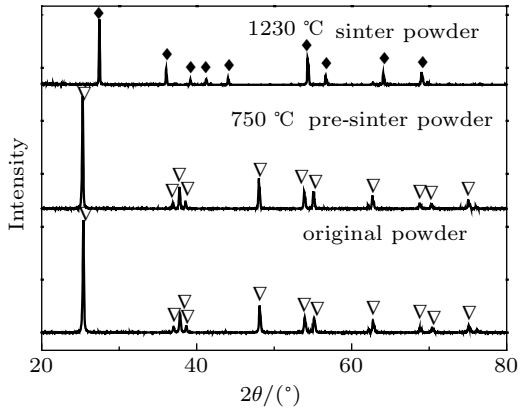


Fig. 2. XRD patterns of TiO_2 ceramic powder: (a) original, (b) 750 °C pre-sintered, and (c) 1230 °C sintered.

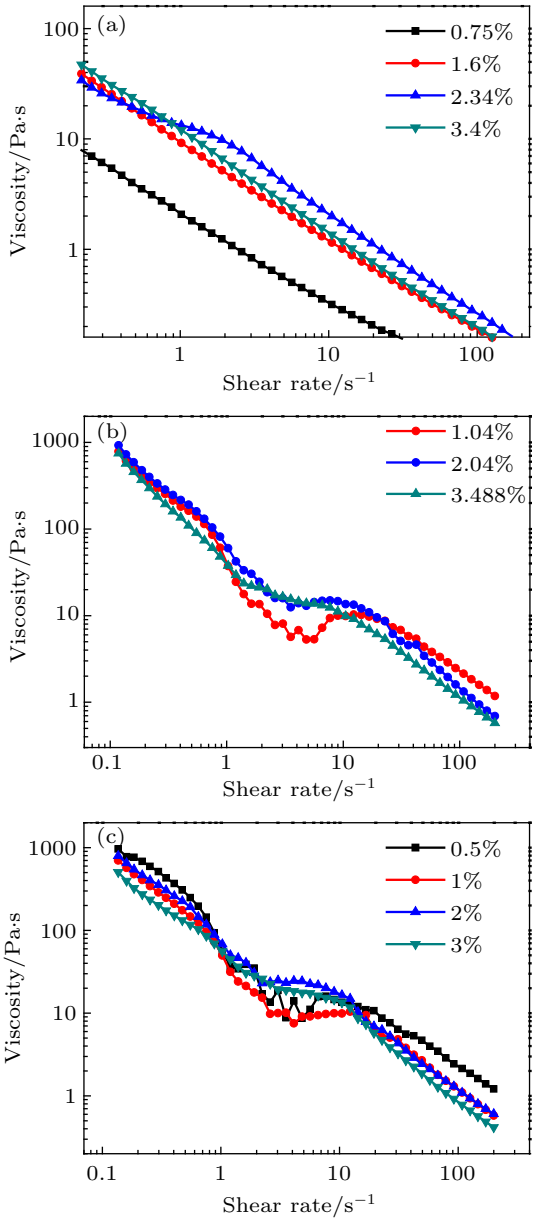


Fig. 3. Viscosity as a function of shear rate of (a) PAA, (b) PEI ($M_w = 600$ g/mol), and (c) PEI ($M_w = 1200$ g/mol).

The selected dispersant molecule, the PEI behaves like a cationic polyelectrolyte, which has primary, secondary, and tertiary amine groups in a ratio $\sim 1:2:1$.[16] Being added to an aqueous PEI solution, the TiO_2 particles' surfaces are coated, and the resulting zeta potential behavior is illustrated in Fig. 4. The bare particles display an isoelectric point around pH = 5.2. The isoelectric point shifts to around pH = 11.77 upon the addition of PEI. Thus, an appropriate pH range should keep away from the range of 10.5–12, because in this scope, the powder is very unstable and easily agglomerates. Therefore, the workable pH range is lower than 10.5. With PEI-coated TiO_2, the slurry dispersed well, and is also very uniform, which is favorable for extrusion in the process of direct writing. In addition, the solid content of slurry can be improved with PEI-coated TiO_2.

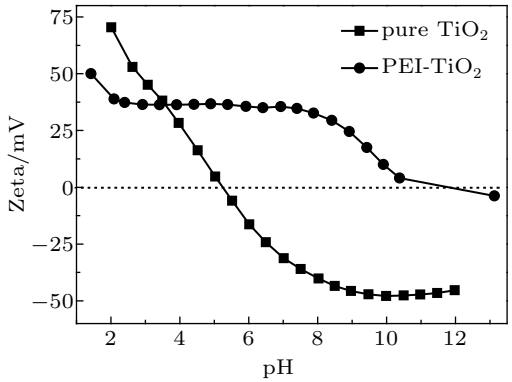


Fig. 4. Zeta potential as a function of pH value for bare and PEI_{600} coated TiO_2 powders dispersed in water. All the tested slurries have the same volume fraction of 1.3%.

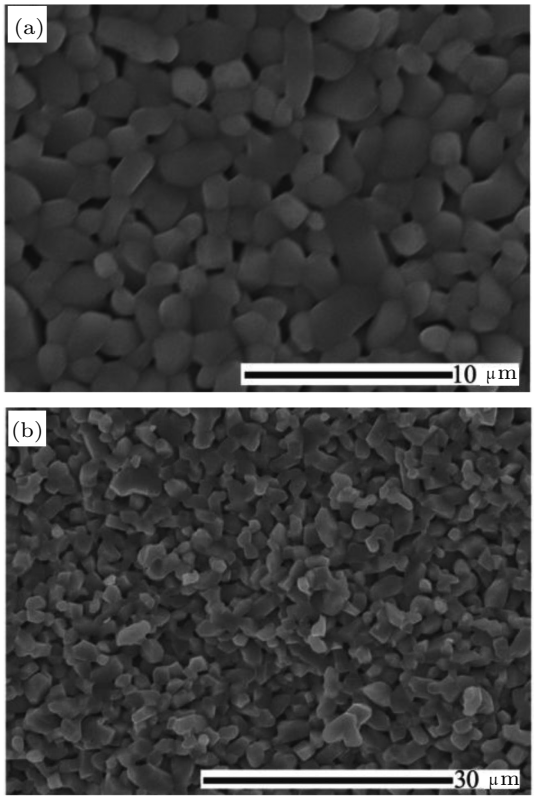


Fig. 5. SEM pictures of (a) surface and (b) cross microstructure of wafers.

Two ceramics wafers are sintered under the same sintering temperature. The surface and cross section are shown in Fig. 5. The dielectric constant is measured to be about 95 from 0.01 GHz to 0.08 GHz, as shown in Fig. 6. The dielectric constant of the three-dimensional rutile TiO_2 woodpile type has an influence on the location of its forbidden band.[17–19]

Many direct-written structures have been done by Smay,[20,21] Lewis[22,23] and Cesarano[24] *et al*. The biggest challenge for the ink is that they must be equipped with self-supporting features that span gaps in the underlying layers. The direct-writing ink must satisfy two features. One is good viscoelastic properties. With this property, the ink can flow through the nozzles under appropriate pressure and recover rapidly after deposition. Another important criterion is that the inks contain a high solids loading, leading to minimal shrinkage and minimal deviation from the expected shape upon drying. It must flow through the nozzle under pressure to form the desired structure. The inks should be neither too dry like solid nor too wet like fluid.

The ink with a solid loading of 42 vol.% was obtained. The storage modulus (G') and loss modulus (G'') of the colloidal gels inks as a function of shear stress are plotted in Fig. 7(a). The apparent viscosity as a function of shear rate is plotted in Fig. 7(b).

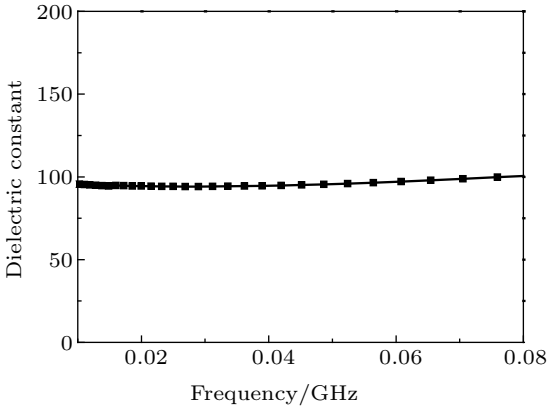


Fig. 6. Dielectric constant of TiO_2 ceramic wafers in the microwave frequency.

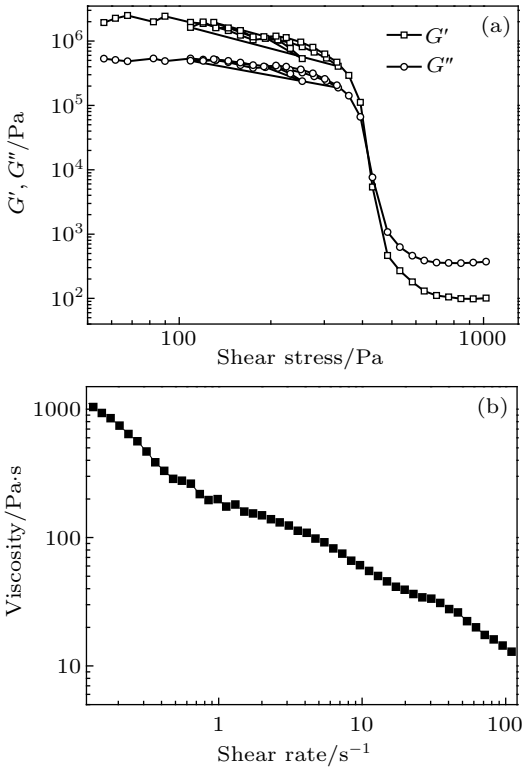


Fig. 7. (a) Shear stress-dependent behavior of storage modulus (G') and loss modulus (G'') for TiO_2 inks at a frequency of 1 Hz. (b) Corresponding plot of apparent viscosity versus shear rate for TiO_2 inks.

As shown in Fig. 7(a), G' keeps a relatively constant value of 10^6 Pa during the shear stress increases from 55 Pa to 400 Pa. Once the shear stress gets higher than 400 Pa, the yield stress G' decreases quickly, which makes it possible for

the Pastes to pass the nozzle smoothly. The storage modulus of the ink is 1×10^6 Pa, which can guarantee the spanning structures. Therefore, the ink is deemed to be successful and desired structures can be achieved. At this solid loading, the inks display a shear thinning behavior, which is shown in Fig. 7(b). This behavior is vital for direct writing, in that the ink can flow smoothly through nozzle during the process. This shear thinning with yield-stress rheology can be described by the Hershel–Bulkley model.[25]

When the given stress is higher than the yield stress, the ink can flow like a fluid; otherwise, it will behave like a solid. Besides, the value of yield stress has an influence on shape retention upon the extrusion. In the case of the TiO_2 ink studied here, polyelectrolyte PAA is used for bridging the flocculation. The interaction between Particles and polyelectrolyte reaction can increase the yield stress of the ink. For the desired concentration inks, the first polymer layer is PEI, and the second polymer is PAA. A PEI molecule will form inter-chain complexes on one side and have a reaction with PAA on the other side. PEI molecules possess many positive sites and are likely to be complex with numerous PAA chain segments.[12]

3D woodpile TiO_2 structures, consisting of 2 units (8 layers), are fabricated. Samples with three different rod diameters and different spacing distances are constructed by direct-writing assembly. Scanning electron microscope (SEM) images of the top surfaces and cross microstructures of sintered TiO_2 woodpile are shown in Fig. 8. It is displayed that these rods were aligned as desired, with excellent self-support and no obvious interruptions or defects. The samples support themselves very well. The deflection of the spanning rods can be described by a model which is described in detail in Ref. [16].

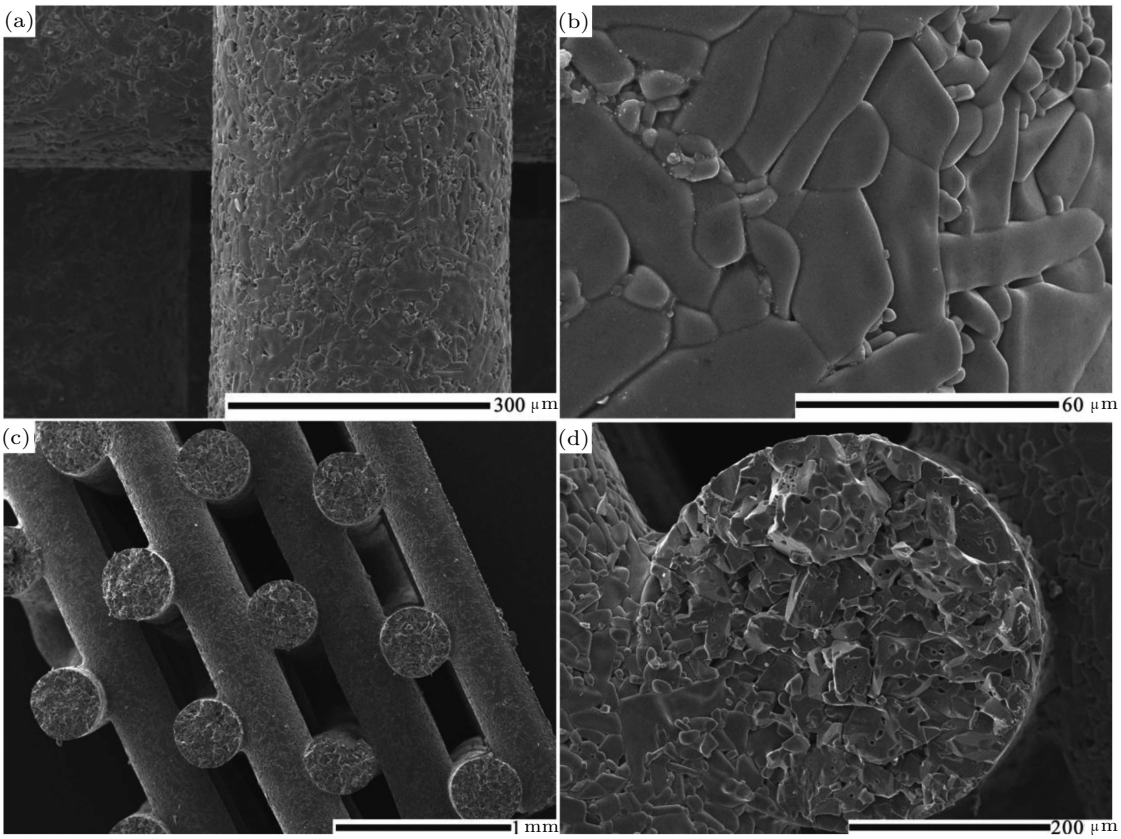


Fig. 8. SEM images of surface of cross sections for a sintered sample: (a) top view of one rod width; (b) top surface microstructure of rod in panel (a); (c) the side view of sintered TiO_2 woodpile; and (d) cross microstructures of one rod in panel (c).

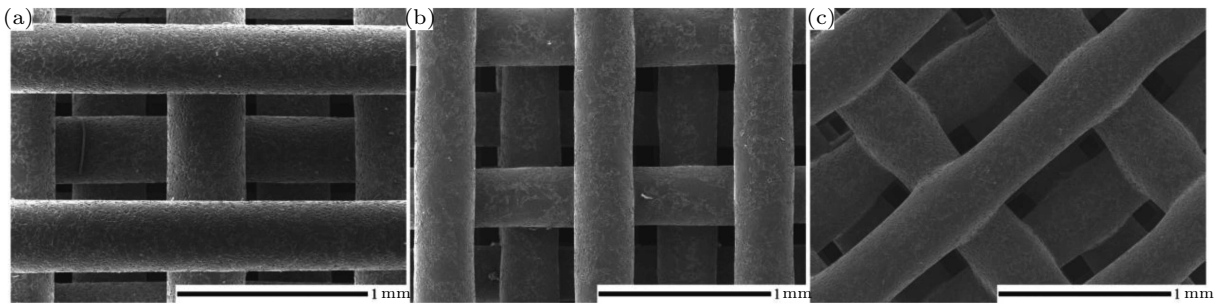


Fig. 9. Top surfaces of characteristic TiO_2 woodpile with (a)–(c) three different rod diameters and different spacings.

Surface morphology and microstructural properties of sintered TiO_2 woodpile are characterized by using SEM (Fig. 9). Three woodpile structures with different in-plane centers to center rod spacings and rod diameters are fabricated. The TiO_2 dielectric constant (ε) of 95 is used in the simulation. The plane wave expansion[26] (PWE) is adopted for computing band gaps. The measurements are indicted in Fig. 10. In the first group, TiO_2 rods (410 μm in diameter) are patterned to create the center gap location of 31 GHz. In the second group, TiO_2 rods (354.8 μm in diameter) are arrayed to create the center gap location of 39.1 GHz. In the third group, TiO_2 rods (413 μm in diameter) are patterned to create the center gap location of 38 GHz. Simulation results based on the plane wave expansion (PWE) method are displayed in Fig. 11. Table 1 shows the numerical results. Comparing the theoretical calculations with the experimental results, they agree well to some extent. It is shown that three measured dips in transmission spectra are the results of EBGs of such structures. On the other hand, this is attributed to disorder in the rod arrangement. Thus, further improving the periodicity of the rod arrangement would help obtain better agreement between the results of theoretical calculation and experimental measurements.

Table 1. Characterization of three groups of woodpile structures, and simulated frequency location results.

Group	Diameter/μm	Period/μm	Center of frequency/GHz
1	410	950	34
2	354	921	42
3	413	1144	32

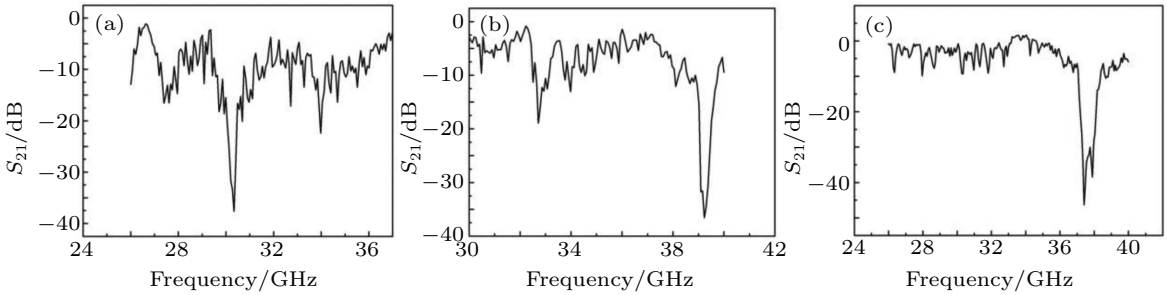


Fig. 10. Electrical measurements of three woodpile structures corresponding to panels (a)–(c) in Fig. 9.

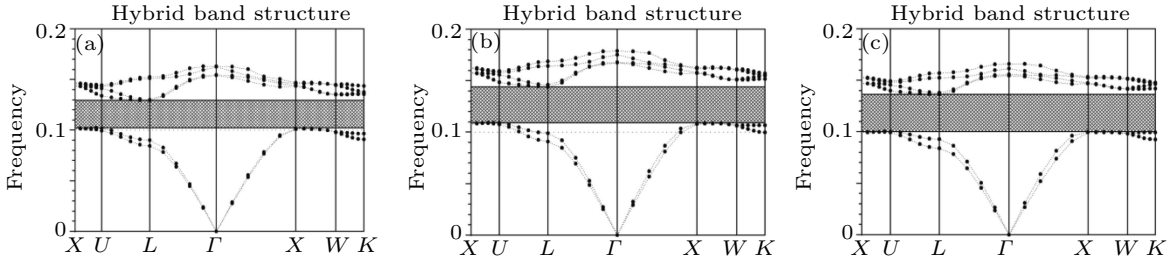


Fig. 11. Simulated electromagnetic gap location of three woodpile structures corresponding to panels (a)–(c) in Fig. 10.

4. Conclusion

A stable, concentrated TiO_2 ink with a solid volume fraction of 0.42 has been developed for the deposition of 3D woodpile structures. Colloidal gel strength was regulated by the addition of a cationic polyelectrolyte for initial dispersion followed by addition of an anion polyelectrolyte for controlling flocculation. The rheological properties of TiO_2 ink were measured to be suitable for the direct writing process. Structures maintained their shapes perfectly and possessed self-supporting features. Sintered samples were obtained in an ordinary air furnace at 1230 ℃ for 4 hours after being dried. The three woodpile structures show a deep gap at 31 GHz, 39.1 GHz, and 38 GHz. The measured microwave characteristics of the results agree well with simulations based on plane wave expansion (PWE).

References

[1] Therriault D, White S R and Lewis J A 2003 *Nat. Mater.* **2** 265
[2] Gratson G M, Xu M J and Lewis J A 2004 *Nature* **428** 386
[3] Chang C E, Tran V H, Wang J B, Fuh Y K and Lin L W 2010 *Nano. Lett.* **10** 726
[4] Lin Y K, Rivera D and Chen K P 2006 *Opt. Express* **14** 887
[5] Lin Y K and Herman P R 2005 *J. Appl. Phys.* **98** 096102
[6] Lin Y, Herman P R and Darmawikarta K 2005 *Appl. Phys. Lett.* **86** 071117
[7] Zhang T H, Piao L Y, Zhao S L, Xu Z, Wu Q and Kong C 2012 *Chin. Phys. B* **21** 118401
[8] Li C Y, Wang J B and Wang Y Q 2012 *Chin. Phys. B* **21** 098102
[9] Zhang S Q 2012 *Chin. Phys. B* **21** 065101
[10] Fan C Z, Wang J Q, He J N, Ding P and Liang E J 2013 *Chin. Phys. B* **22** 074211
[11] Miranda P, Saiz E, Gryn K and Tomsia A P 2006 *Acta Biomater.* **2** 457
[12] Nadkarni S S and Smay J E 2006 *J. Am. Ceram. Soc.* **89** 96

[13] Dietrich A and Neubrand A 2001 *J. Am. Ceram. Soc.* **84** 806
[14] Alemdar A, Öztekin N, Güngör N, Ece Ö I and Erim F B 2005 *Colloids. Surf. A Physicochem. Eng. Asp.* **252** 95
[15] García-Santamaría F, Xu M, Lousse V, Fan S, Braun P V and Lewis J A 2007 *Adv. Mater.* **19** 1567
[16] Smay J E, Gratson G M, Shepherd R F, Cesarano J and Lewis J A 2002 *Adv. Mater.* **14** 1279
[17] Sözüer H and Dowling J P 1994 *J. Mod. Opt.* **41** 231
[18] García-Santamaría F, Xu M, Lousse V, Fan S, Braun P V and Lewis J A 2007 *Adv. Mater.* **19** 1567
[19] Maldovan M, Thomas E L and Carter C W 2004 *Appl. Phys. Lett.* **84** 362
[20] Zhu C and Smay J E 2012 *J. Mater. Process. Technol.* **212** 727
[21] Xie B J, Parkhill R L, Warren W L and Smay J E 2006 *Adv. Funct. Mater.* **16** 1685
[22] Lewis J A, Smay J E, Stuecker J and Cesarano J 2006 *J. Am. Ceram. Soc.* **89** 3599
[23] Gratson G M, García-Santamaría F, Lousse V, Xu M, Fan S, Lewis J A and Braun P V 2006 *Adv. Mater.* **18** 461
[24] Cesarano J, Aksay I A and Bleier A 1988 *J. Am. Ceram. Soc.* **71** 250
[25] Huang X and Garcia M H 1998 *J. Fluid Mech.* **374** 305
[26] Ho K, Chan C and Soukoulis C 1990 *Phys. Rev. Lett.* **65** 3152